International Journal of Computer Engineering in Research Trends
ISSN: 2349-7084/https://doi.org/10.22362/ijcert/2025/v12/i2/v12i201
Volume 12, 2, February 2025

Research Paper

An Artificial Intelligence Model for Predicting Flooding and Drought in Bali Local Government Area of Taraba State, Nigeria

Onesimus John Waino [1*], Steven David [2]

[1,2] *Computer Engineering Department Federal Polytechnic Bali, Taraba State, Nigeria.*
[2]*davidsteven41@gmail.com.*

**Corresponding Author: onesimus10103@bazeuniversity.edu.ng*

Received: 12/10/2024 Revised: 26/12/2024 Accepted: 23/01/2025 Published: 28/02/2025

Abstract: - The ability to predict climate-induced phenomena like drought and flooding are critical for effective resource management and mitigation planning. This study investigates the application of advanced predictive models to forecast drought and flood indices using comprehensive meteorological datasets from Meteomatics' global weather monitoring platform. The dataset, spanning 14 years (2010–2024) for Bali, Taraba State, Nigeria, comprises over 5,000 data points and 33 climate variables. Data preprocessing included temporal sorting, duplicate removal, and missing value imputation through interpolation and forward-fill methods. Correlation analyses highlighted significant relationships among key features, such as temperature, humidity, wind speed, and solar energy, which play pivotal roles in drought and flooding dynamics. For predictive modeling, six approaches—ARIMA, SARIMA, Prophet, XGBoost, Random Forest, and LSTM—were evaluated across five targets: Standardized Precipitation Index (SPI), Standardized Precipitation Evapotranspiration Index (SPEI), daily water balance, 30-day water balance, and SPEI-30d. The models underwent rigorous optimization through feature selection and hyperparameter tuning. Results revealed that machine learning models, particularly Random Forest and XGBoost, outperformed traditional statistical methods and neural networks in most scenarios, with XGBoost achieving an impressive R^2 of 0.843 for SPEI predictions. Prophet proved most effective for daily water balance predictions, while Random Forest excelled in 30-day water balance and SPEI-30d forecasting. This study underscores the critical importance of model optimization in enhancing predictive accuracy and demonstrates the potential of machine learning models for addressing complex hydrological forecasting challenges. The findings provide a robust framework for drought and flood prediction, contributing to improved water resource management and disaster preparedness strategies.

Keywords- Machine learning, AI models, Drought prediction, flood forecasting.

---

1. Introduction

The increasing frequency and severity of extreme weather events, such as floods and droughts, represents an ongoing problem increasingly globally driven by climate change [1]. These situations pose serious risks in areas such as Bali Local Government Area of Taraba State, Nigeria. Located within a semi-arid zone, serving as a major agricultural crop producer in the state and beyond, the region is particularly vulnerable to extreme weather events, which cause significant damage to the social, economic and environmental impact. Severe floods have caused loss of property and lives, and recurring droughts disrupt agricultural production and water resources management.

The vulnerability of households in Taraba State to food insecurity is further aggravated by extreme weather events including recurrent droughts. Research shows that 92% of households in the state are food insecure. The households affected by climate shocks such as droughts even fall into the very low food security category [2]. Droughts significantly reduce agricultural productivity as they result in lower crop yields, impaired livestock health and rising food prices, which in turn limit food availability, access and utilization. To address these challenges, effective agricultural management strategies must be implemented that emphasize community engagement, timely intervention and capacity building to enhance resilience to climatic adversities.

The main research problem revolves around the inability of the existing predictive system to provide precise, timely, and localized forecasts that could facilitate proactive disaster response measures. Traditional statistical methods often fail to capture the non-linear and dynamic nature of climate change and the environmental changes, thus further emphasizing the need for innovative approaches [3]. This study directly addresses this gap by proposing a learning-driven artificial intelligence (AI) model designed to predict droughts and floods in Bali Local Government Area of Taraba State with the highest accuracy.

The AI model leverages robust datasets from the Meteomatics global weather monitoring platform, which includes more than 5,000 data points in 33 climate variables covering 14 years (2010–2024). Using machine learning algorithms such as XGBoost, Random Forest, and Long Short-Term Memory (LSTM), this study optimizes predictive accuracy for key hydrological indices, such as the Standardized Precipitation Index (SPI) and Standardized Precipitation Evapotranspiration Index (SPEI).

With its ability to provide actionable insights, the model addresses critical disaster preparedness challenges in a localized setting, providing significant implications for early warning systems, community resilience, and resource management. Specifically, by providing information on extreme events such as droughts and floods, the model empowers the local government and community members to implement targeted interventions, such as early intervention, improved irrigation practices, and resource allocations.

Key Contributions of the Research

This research fills key gaps in the application of advanced AI-based prediction (ML) models to disaster prediction in resource limited settings. The main contributions are:

1. **Academic Contribution**: By optimizing and developing ML models, this study enriches the general knowledge base of predicting predictive weather in developing regions (Ojo & Akinyemi, 2023).
2. **Policy implications**: This research can provide actionable insights for disaster management, helping policymakers allocate resources more efficiently and reduce disaster losses.
3. **Technological Innovation**: It shows the importance of combining traditional models with advance machine learning techniques, which can be used in similar settings around the world.
4. **Societal Impact**: Enhanced predictive accuracy can lead to better preparedness, floods and droughts can be avoided or reduced in and around Taraba State thereby reducing socio-economic disadvantages.

2. Literature Survey

This chapter reviews the existing literature on the use and application of machine learning (ML) techniques for flood prediction and drought, focusing on the scope, challenges and gaps of research. Recent developments in machine learning models, from traditional statistical methods to advance deep learning frameworks, is discussed to provide a general understanding of its applicability in the context of Taraba State, Nigeria and similar regions.

2.1 Review of Related Studies

Machine learning techniques have revolutionized predictive modeling in climate science, offering greater accuracy and scalability. These models address critical issues in flood and drought forecasting, such as nonlinearity and the interaction between climate change.

2.1.1 Traditional Machine Learning Techniques.

Statistical models such as Autoregressive Integrated Moving Average (ARIMA) and Seasonal ARIMA (SARIMA) are the mainstay of seasonal forecasting. Studies such as Hyndman and Athanasopoulos (2018) highlight its importance in capturing linear trends and trends over time. However, this method relies on stability issues limiting its application to dynamic environments such as Sub-Saharan Africa [4].

Ensemble learning techniques, such as Random Forest (RF) and XGBoost, are widely used for flood forecasting, known for its robustness against overlifting and its ability to handle heterogeneous data [5] . For example, [6] found a 15% improvement in prediction accuracy compared to traditional statistical models when they analyzed flood risk in Nigeria using RF and XGBoost.

2.1.2 Advanced Deep Learning Techniques

Deep learning models, especially Long Short-Term Memory (LSTM) networks, are excellent for data modeling based on sequence and time series. The research by [7] in Rwanda demonstrated the ability of LSTM to predict water flow with minimal error and overcame the limitations of simpler models such as ARIMA.

AI models can achieve high accuracy in predicting flooding and drought events. For example, a study by [8] found that a convolutional neural network (CNN) model was able to predict flooding events with an accuracy of 95%.

AI models can be used to predict flooding and drought events at different lead times. For example, a study by[9] found that an AI model was able to predict flooding events up to 72 hours in advance.

AI models can be used to predict flooding and drought events in a variety of geographical regions. For example, a study by [10] found that an AI model was able to predict drought events in both arid and tropical regions.

Furthermore, Convolutional Neural Networks (CNNs) and hybrid approaches combining CNNs and LSTMs have shown promise in capturing spatiotemporal dependencies in weather data [11]. These methods are particularly useful in areas with difficult terrain such as Taraba State.

2.1.3 Applications in Sub-Saharan Africa

In sub-Saharan Africa, the use of machine learning for weather forecasting is relatively new but promising. Studies such as [12] have used Gaussian kernel data and remote sensing data to estimate drought severity, showing the relationship between ML model to address data scarcity. Similarly, [13] used neural network-based model to forecast flood risk thereby enabling more targeted humanitarian response.

2.2 Research Gaps.

Several gaps remain in the current study of climate formation in Sub-Saharan Africa, including the lack of regional customization for unique situations such as those in Taraba State [14] , lack of weather high quality weather data [15], limited comparative analysis of traditional and ML models, higher demand for advanced model development

[16], and inadequate integration of socio-economic factors to ensure adequate and practical application.

2.3 Recent Trends and Future Directions

Recent advancements in machine learning include concepts such as transfer learning and federated learning, which show potential to address some of the problems. Transfer learning has been shown to be effective in fine tuning data for data scarce context like Taraba State using pretrained models developed in data rich regions.[17]. In similar manner, federated learning enables collaborative model learning to be performed across multiple decentralized datasets, which reduces the complexity of the data and improves the data accuracy.

Integrating explanatory AI (XAI) measures is another emerging trend. XAI provides additional insights that will help practitioners understand the meaning of model insights and thus increase trust and acceptance among policy makers [18].

The literature presents the insights of machine learning for flood and drought prediction. However, to achieve better results requires addressing regional data limitations, ensuring computational feasibility and integrating socio-economic development is more important. The focus of this study in Bali Local Government Area of Taraba State, Nigeria provides an opportunity to provide new insights into the field with the comparison of traditional and advance ML models and developing an AI Model for drought and flood prediction ultimately improving disaster preparedness and resource efficiency in the region.

3. Methodology

The methodology outlines the systematic approach undertaken in this study to predict flooding and drought in Bali Local Government Area, Taraba State, Nigeria. It involves an in-depth exploration of the study area, comprehensive data collection, and the application of machine learning models tailored to optimize prediction accuracy.

3.1 Study Area

Bali local government area is one of the 16 Local Government Areas of Taraba state, Nigeria, it covers a total land area of about 9,146km^2 and extends between latitude 7^{o}30' 00" to 8^{o}10'00" North of the Equator and 5^{o}45' 00" to 6^{o}15'00" East of the Greenwich meridian [19] .

3.2 Data Collection and Preparation

Data Source: Data was acquired from the Meteomatics global weather monitoring platform which provides comprehensive weather, environmental and climate data through its robust APIs.

Meteomatics, a weather data collection tool, provides high-quality weather information by combining multiple sources. These include global climate models such as ECMWF and GFS for key datasets, National services such as MeteoSwiss and DWD for local forecasts, satellite and radar data for surveillance in real-time (such as cloud and storm tracking), in-situ measurements from land, sea, and atmosphere for accurate coverage, and long-term climate models such as CMIP6 for projections to the year 2100.

Metadata and Data Nomenclature: The data sets were extracted based on the BALI location in Taraba state, Nigeria. Features cutting across climatic, meteorological , environmental and Agricultural categories were carefully selected to cover a wider scope and balance for the prediction model. This so that the model won't be blindsided to just a few categories that may pass for drought and flooding enablers. The dataset covered a 14-year (2010 - 2024) duration.

Variable/Feature descriptions: The dataset features a wide array of daily and hourly weather attributes essential for understanding climate phenomena. Key variables include cloud cover percentage, local temperature, relative humidity, and precipitation details like type, volume, and coverage. Temporal attributes, such as date and time (in ISO 8601 format), are standardized to UTC using epoch-based calculations. Solar radiation, UV index, wind parameters (speed, direction, gusts), and visibility are also included to capture the full scope of meteorological conditions. Additional data points, such as moon phases, sunrise/sunset times, and station-based historical observations, provide further granularity.

Precipitation-specific metrics include probabilities, coverage, and snow-related parameters, alongside atmospheric pressure values expressed in millibars. For forecasting purposes, normal arrays represent statistical summaries of weather data over specific periods, offering mean, maximum, and minimum values. This comprehensive dataset integrates real-time, historical, and forecasted observations, ensuring robust inputs for predictive modelling and analysis.

Overall, the combination of diverse climatic, temporal, and spatial features in this dataset enables nuanced exploration of weather dynamics. This structured approach lays a solid foundation for developing and validating predictive models for drought and flooding in Bali Local Government Area.

3.3 Data Pre-Processing Steps

Firstly, in general, date sorting needed to be done across all the data batches, from the original ISO format to the datetime format, then the whole batches were merged and sorted based on the date/time variable. Furthermore, duplicates were checked for and removed based on the datetime column and the index reset to normal. The result of this initial pre-processing step as seen in the fig below contains 5,279 rows and 33 features/variables.

```
Data columns (total 33 columns):
 #   Column            Non-Null Count  Dtype
---  ------            --------------  -----
 0   name              5279 non-null   object
 1   datetime          5279 non-null   datetime64[ns]
 2   tempmax           5279 non-null   float64
 3   tempmin           5279 non-null   float64
 4   temp              5279 non-null   float64
 5   feelslikemax      5279 non-null   float64
 6   feelslikemin      5279 non-null   float64
 7   feelslike         5279 non-null   float64
 8   dew               5279 non-null   float64
 9   humidity          5279 non-null   float64
 10  precip            5279 non-null   float64
 11  precipprob        5279 non-null   int64
 12  precipcover       5279 non-null   float64
 13  preciptype        3135 non-null   object
 14  snow              3453 non-null   float64
 15  snowdepth         3453 non-null   float64
 16  windgust          3453 non-null   float64
 17  windspeed         5279 non-null   float64
 18  winddir           5279 non-null   float64
 19  sealevelpressure  3453 non-null   float64
 20  cloudcover        5279 non-null   float64
 21  visibility        887 non-null    float64
 22  solarradiation    5279 non-null   float64
 23  solarenergy       5279 non-null   float64
 24  uvindex           5279 non-null   int64
 25  severerisk        887 non-null    float64
 26  sunrise           5279 non-null   object
 27  sunset            5279 non-null   object
 28  moonphase         5279 non-null   float64
 29  conditions        5279 non-null   object
 30  description       5279 non-null   object
 31  icon              5279 non-null   object
 32  stations          5279 non-null   object
dtypes: datetime64[ns](1), float64(22), int64(2), object(8)
```

Fig. 1: A summary of the data

From the above data summary, it is easily noticeable that some of the variables have missing values, which were treated using specialized approaches that fitted the nature of our study (time series forecasting).

Data cleaning: In this section more emphasis was placed on solving the missing value issues on 5 key features as follows:

1. Temperature(minimum, maximum, and mean temperatures)
2. Extended periods of sunshine hours
3. High relative humidity.
4. Low wind speeds
5. High evapotranspiration.

Most of the wind and precipitation features also had over 30% of missing values but a few of the heat/solar based features had as many as 90% missing. Two separate methods were used to handle the missing values:

a. **The Interpolation method**: This technique assumes that the missing data can be filled in by applying the principles of straight-line geometry to the available data points. This was done on variables that have continuous data points like temperature and wind speed, where gaps in the data were managed smoothly, a necessity for making reliable projections [20] .

b. **The forward fill method**: In this approach, missing values are filled based on the last valid observation, and such approach has worked well in maintaining continuity of the weeks filled by numerical weather stations and sensors.

In our case, we separated the data into numerical and categorical batches and then applied the forward fill approach to the categorical section and applied the interpolation to the numerical features, achieving a complete fill and less zero or null fills.

4. Exploratory and Statistical Data analysis

4.1 Analyzing Wind Features:

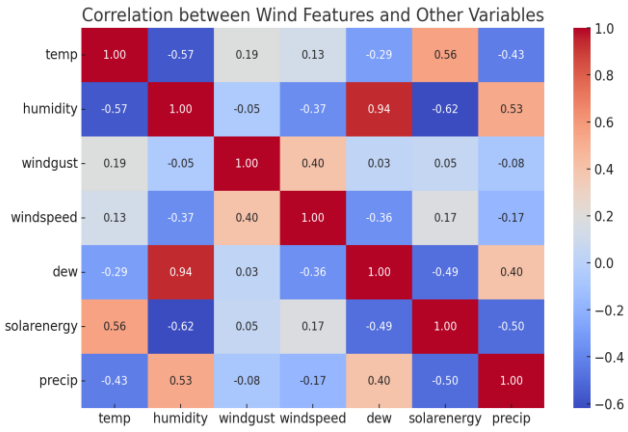

Fig. 2: Correlation between wind features and other variables.

The analysis reveals distinct relationships between various weather factors in Bali. Wind speed and wind gust exhibit a fair positive correlation (r = 0.40), indicating that higher wind speeds are often accompanied by intense gusts, potentially contributing to violent weather events. Humidity and dew point demonstrate a very strong positive correlation (r = 0.94), underscoring their mutual reliance on air moisture and their influence on heavy rainfall occurrences.

Precipitation shows a low negative correlation with both wind speed (r = -0.17) and wind gust (r = -0.08), suggesting that stronger winds do not necessarily result in higher precipitation, though this relationship may vary with different weather systems. Solar energy is weakly correlated with wind speed and wind gust but exhibits an inverse correlation with precipitation (r = -0.50), indicating that higher rainfall reduces solar energy availability.

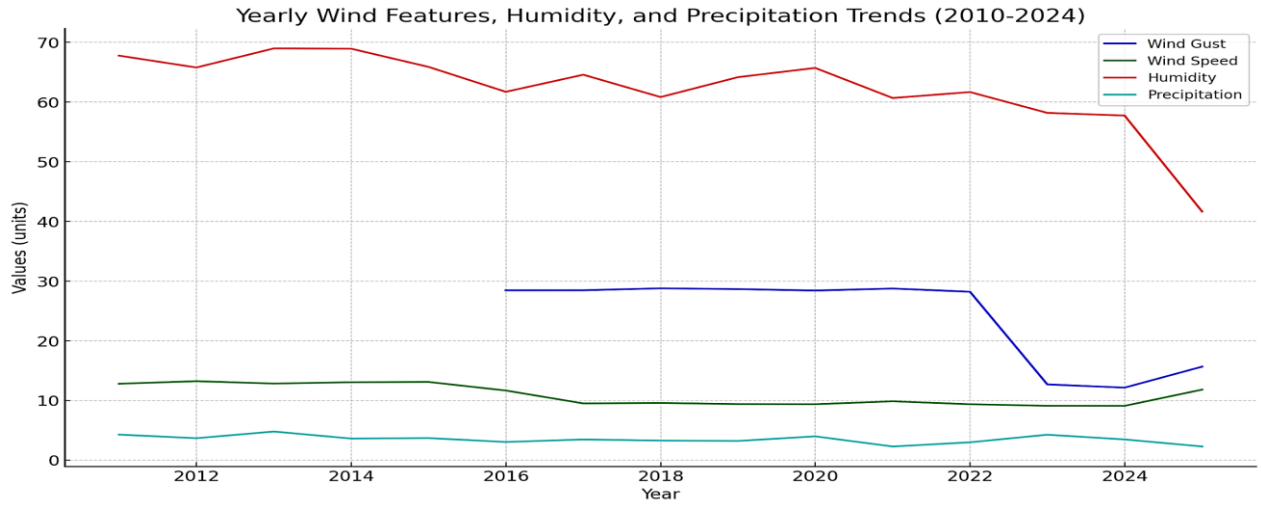

Fig. 3: Wind trends in relationship to humidity and precipitation in Bali between 2010-2014.

Analysis shows dramatic changes in wind gust, with a significant decrease since 2021, although wind speed has remained relatively stable. These factors along with changes in precipitation and humidity play a role in influencing drought and flooding. Strong winds gust during storms can exacerbate flooding by increasing water levels in certain areas, thereby causing coastal erosion. Conversely, the reduction in humidity year-on-year with exception of 2024, signals drier conditions that increases the risk of drought, especially when combined with low wind activity.

The outlook for solar energy shows modest but steady growth towards 2024, potentially increasing evaporation and land drying and adversely contributing to drought conditions. In Bali, the combination of declining humidity, stable or rising solar radiation, and unstable wind patterns presents a unique and complex scenario. Although diminished wind activity may cause reduction in rainfall, prolonged gust during storm can still trigger flash flooding in coastal and low areas. All these factors suggest that Bali is likely to become more prone to hight risk of drought in the coming years, coupled with the possibility of high localized flooding during intense storms.

4.2 Analyzing temperature features:

Drought/Flooding Indices: There may be risks of droughts when there are high temperatures coupled with low levels of rainfall and humidity whereas flooding potentially low temperatures with a lot of rains could imply flooding risk(Kevin E., 2011).

Temperature Variables: The correlation between tempmax and tempmin is somewhat low (0.23), which indicates that these variables do not move together.

High tempmax and high feltlike pictures are a high degree of correlation (0.75) as it is expected that the higher the temp, the higher is the feels like temperature.

Dew Point and Humidity: The correlation between dew and humidity is high (0.94), and this is expected since dew point is the indicator of how much moisture there is in the air.

There is a strong negative correlation (-0.80) between tempmax and humidity, which means higher temperatures are likely to have lower humidity levels, an important factor in drought conditions.

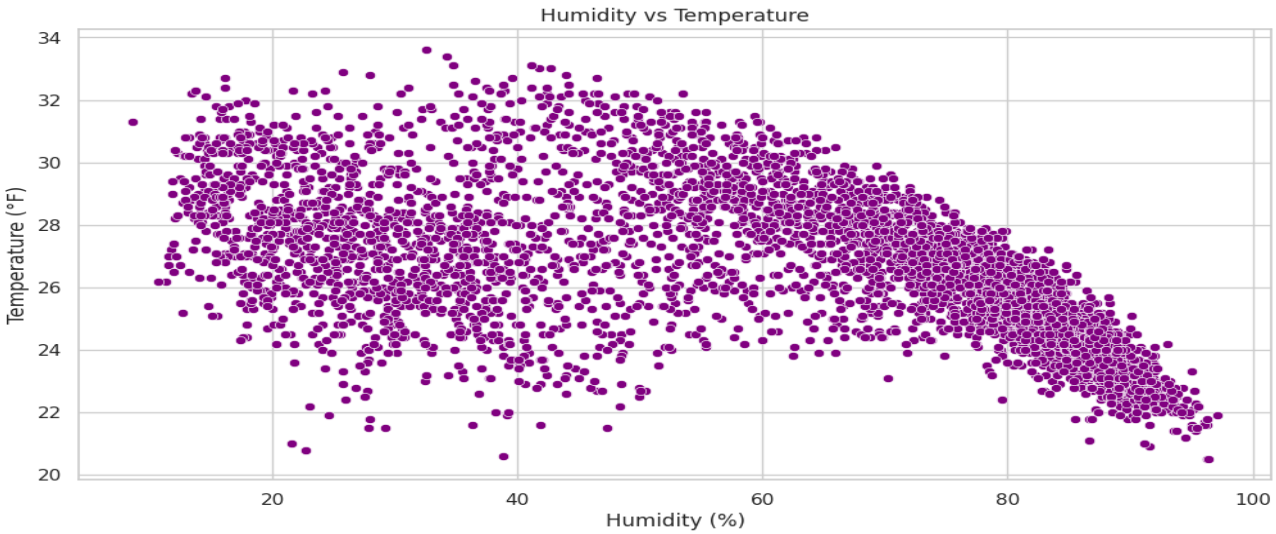

Fig 4: Showing relationship between maximum temperature and humidity

Precipitation: There is an inverse relationship between precip and tempmax (-0.51) as well as temp (-0.43), implying that the increase in temperature is associated with reduction in rainfall. There is a positive correlation between rainfall and humidity (0.53) which suggests that high humidity would increase the chances of rainfall which could lead to flooding

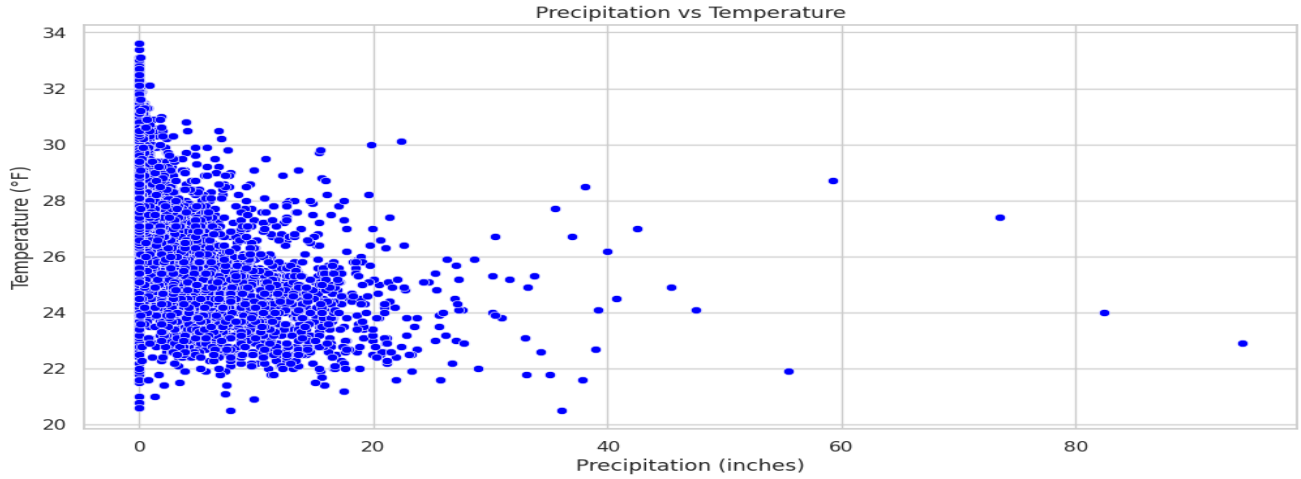

Fig. 5: Relationship between maximum temperature and precipitation

Solar Energy: Solar energy has a positive correlation with tempmax (0.71) and a negative correlation with precip (-0.50), meaning that high solar energy promotes high temp and low precipitation which enhances drought.

4.3 Analyzing Seasonality and key trends across time

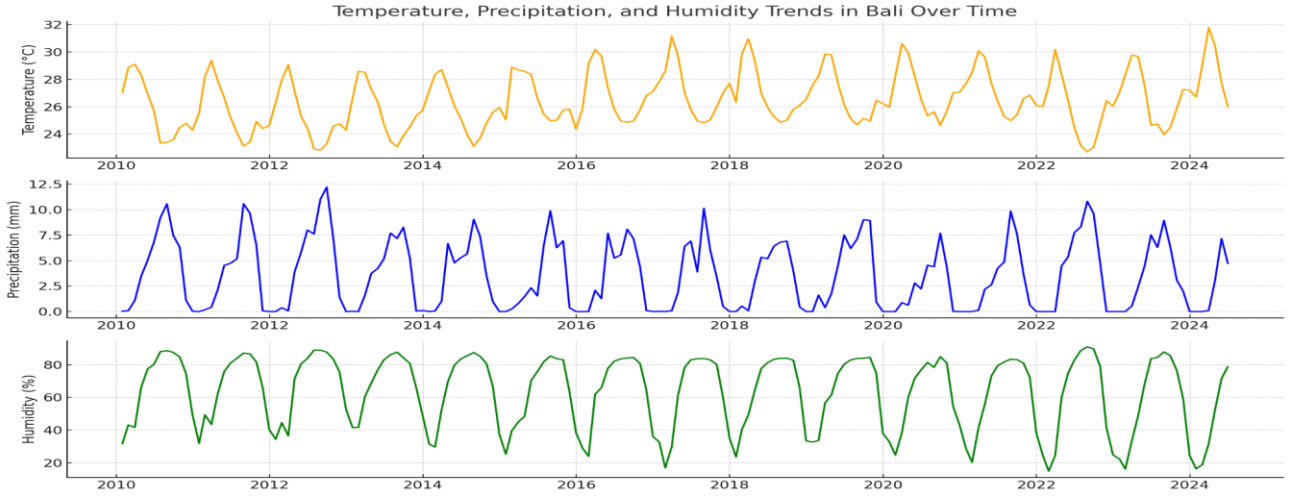

Fig. 6: Time series plots, revealing several key trends in Bali's climate data.

The average temperature follows a sinusoidal seasonal pattern, with long-term warm periods increasing risk of drought, especially during periods of low rainfall. The rainfall pattern reflects the different wet and dry seasons, with heavier rainfall in certain months this increases the chances of flooding because of high humidity. Changes in humidity are proportional to rainfall, with higher humidity often increasing rainfall.

4.4 Exploring Environmental Variables

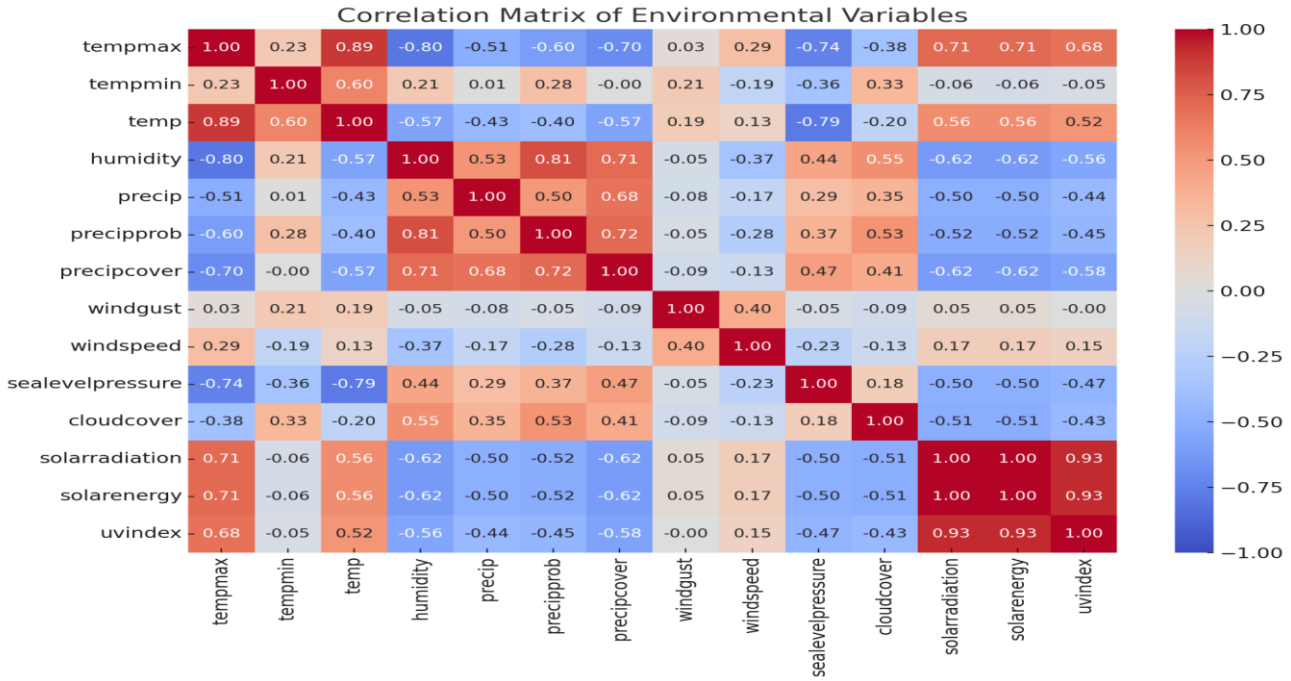

Fig. 7: The correlation matrix highlights relationships between key environmental variables.

Precipitation shows a moderate positive correlation with its likelihood and coverage, indicating a consistent relationship between actual and perceived precipitation. Temperature has a somewhat negative correlation with precipitation and humidity, so higher temperatures can reduce precipitation and humidity, which can lead to drought. In addition, solar radiation and energy are negatively correlated with cloud cover and precipitation, which decreases solar exposure on rainier and cloudier days.

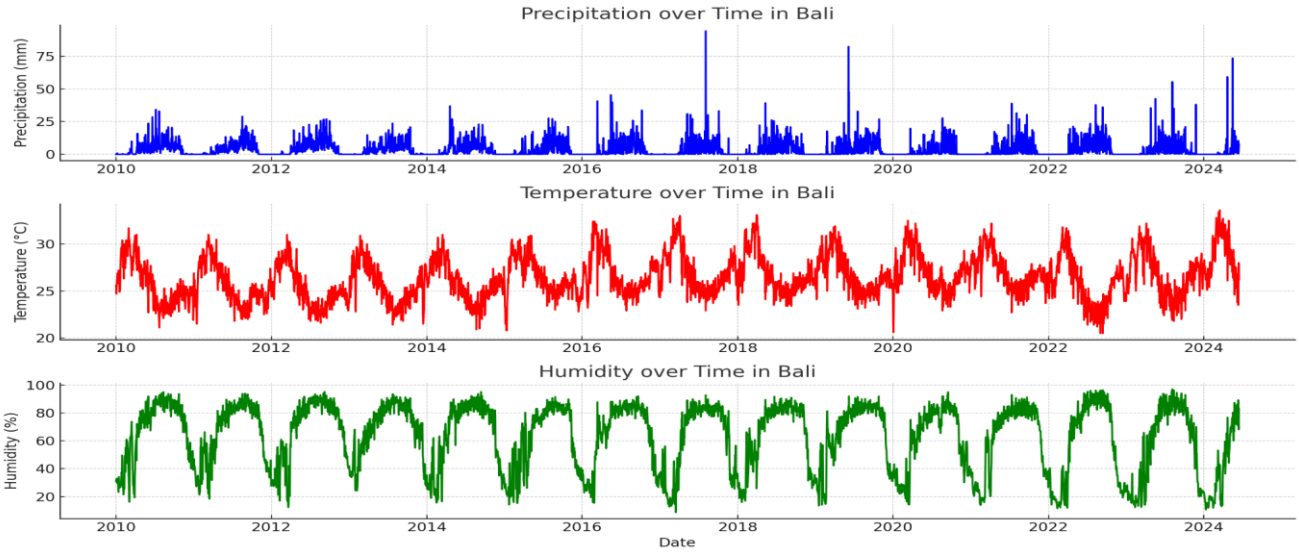

Fig. 8: The time series plots displaying the key trends

4.5 Calculating PET SPI, SPEI

Of the Hargreaves-Samani, Thornthwaite, Priestley-Taylor and Penman-Monteith methods, the Penman-Monteith method is the most preferred and academically and professionally endorsed method for estimating potential evapotranspiration (ET) due to its integrative energy and aerodynamic components and its approach towards accuracy.

The Penman-Monteith Equation: The Penman-Monteith equation can be expressed as:

$$ET = \frac{0.408\Delta(R_n - G) + \gamma \frac{900}{T+2\tau^3} u_2 (e_s - e_a)}{\Delta + \gamma(1 + 0.34u_2)}$$

Where:

- ET = Evapotranspiration (mm/day)
- Net Radiation (Rn): The net amount of radiation energy available at the crop surface.
- Soil Heat Flux (G): The amount of heat absorbed or released by the soil.

- Slope of the Vapor Pressure Curve (Δ): Represents how quickly saturation vapor pressure changes with temperature.
- Psychrometric Constant (γ): Accounts for the energy required to convert water from liquid to vapor.
- Wind Speed (u2): Influences the rate of vapor transport away from the surface.
- Vapor Pressure Deficit (es - ea): Difference between the saturation vapor pressure and actual vapor pressure.

The reasons for the Recommendation and adoption for this project include Accuracy and Comprehensive Approach, Standardization, Scientific Validation, Flexibility and Adaptability.

4.5.1 Calculating Standard Precipitation Index (SPI)

The Palmer Drought Severity Index (PDSI), developed by McKee, Doesken, and Kleist in 1993, assesses wet or dry conditions based on precipitation data, obtained using Standardized Precipitation Index (SPI) over a wide range of time scales (sub-seasonal to interannual). The SPI accounts for precipitation skewness by fitting data to a simple curve and can measure drought impacts over both short (e.g., soil moisture) and longer time scales (e.g., ground water and reservoirs). It measures the frequency or magnitude of drought over intervals of about 3, 6, 12, 24, and 48 months, giving flexible insights into water resource impact (NASA, 2023).

Table. 1: SPI reference interpretation table (NASA, 2023)

SPI	Cumulative Probability	Interpretation
-3.0	0.0014	extremely dry
-2.5	0.0062	extremely dry
-2.0	0.0228	extremely dry (SPI < -2.0)
-1.5	0.0668	severely dry (-2.0 < SPI < -1.5)
-1.0	0.1587	moderately dry (-1.5 < SPI < -1.0)
-0.5	0.3085	near normal
0.0	0.5000	near normal
0.5	0.6915	near normal
1.0	0.8413	moderately wet (1.0 < SPI < 1.5)
1.5	0.9332	very wet (1.5 < SPI < 2.0)
2.0	0.9772	extremely wet (2.0 < SPI)
2.5	0.9938	extremely wet
3.0	0.9986	extremely wet

4.5.2Calculating Standard Precipitation Evapotranspiration Index (SPEI)

The Standardized Precipitation Evapotranspiration Index (SPEI) is a multidimensional and statistically robust drought index suitable for detecting, monitoring and analyzing drought in different contexts, climate and geographical locations. It accurately measures drought severity, duration and intensity while estimating potential evapotranspiration (PET), making it a more useful tool for describing drought severity than traditional indexes such as SPI and sc-PDSI (SPEI.CSIC, 2023).

Calculation of SPEI:

Water Balance Calculation: The first step in calculating SPEI is determining the water balance, which is the difference between precipitation (P) and potential evapotranspiration (PET):

D=P−PETD = P - PETD=P−PET

Where: DDD is the water balance.

PPP is the precipitation. PETPETPET is the potential evapotranspiration.

Water balances are aggregated over different time periods (e.g., 1, 3, or 12 months) to capture different drought conditions. This data is fitted to a probability distribution (usually Gamma or Pearson Type III) and converted to a standardized index (SPEI) using the inverse normal function, allowing spatial and temporal comparisons.

Assessment of Negative Water Balance and Its Effects for Flooding and Drought: The water balance equation (Precipitation − Evapotranspiration) measures the difference between water intake and loss in a system, which influences the health of ecosystems, agriculture, and hydrology.

Positive water balance indicates availability of excess water, benefits soil fertility, redistribution of underlying water soils, rivers, and ecosystems, although excess water can cause flooding or erosion of crops.

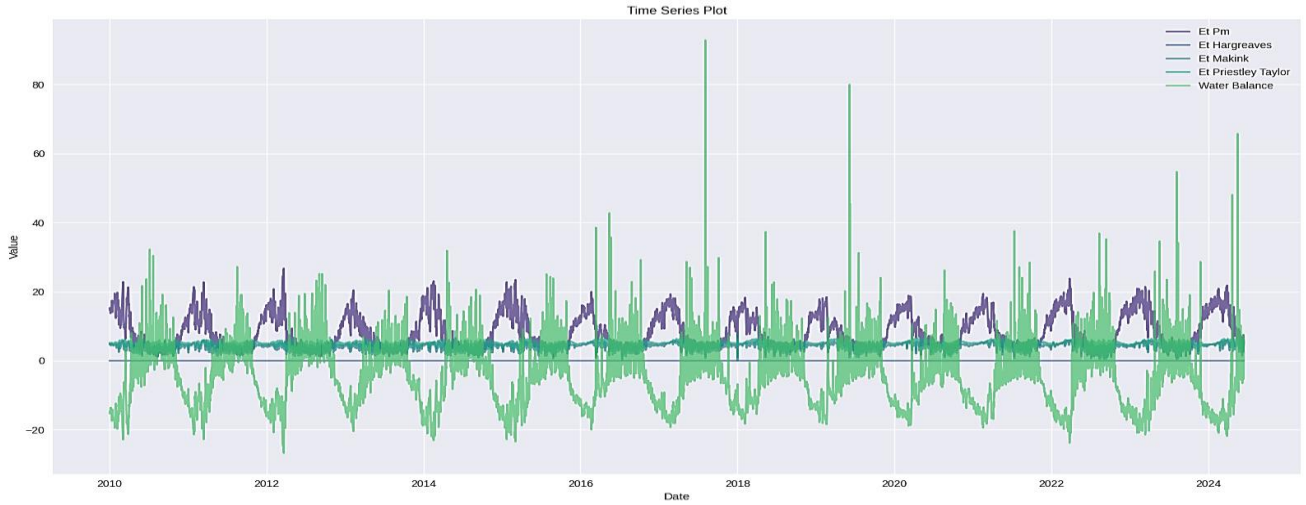

Fig. 9: Time series comparison across all PET methods in relationship to water balance

A negative water balance occurs when evaporation and transpiration is more than precipitation, leading to water shortages. This can reduce soil moisture, reduce groundwater levels, reduce river flows, and exacerbate drought. It affects agriculture by stressing plants, reducing yields, and causing crop failures. Ecosystems also suffer, with plants and animals stressed or extinct, and drought increases wildfire risk because the water in the grass is less.

Understanding water balance helps in resource management, agriculture, and environmental protection. It helps regulate water, conserve water, and supports ecosystems. Urban planners also use this information to develop water plans for cities, for sustainable development and thus better monitor water shortages or surpluses.

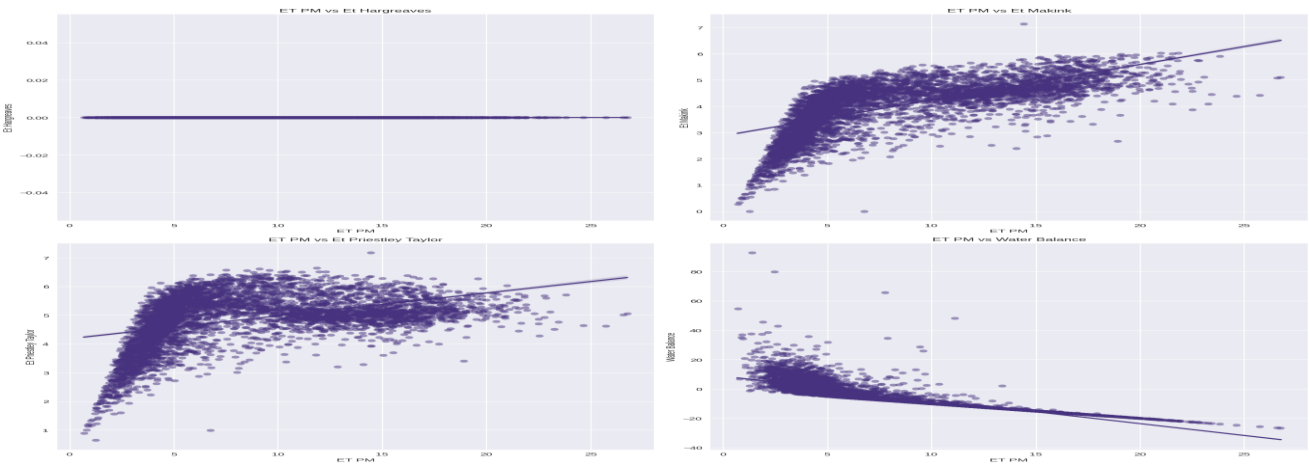

Fig. 10: Showing linear relationships between all PET methods and the water balance

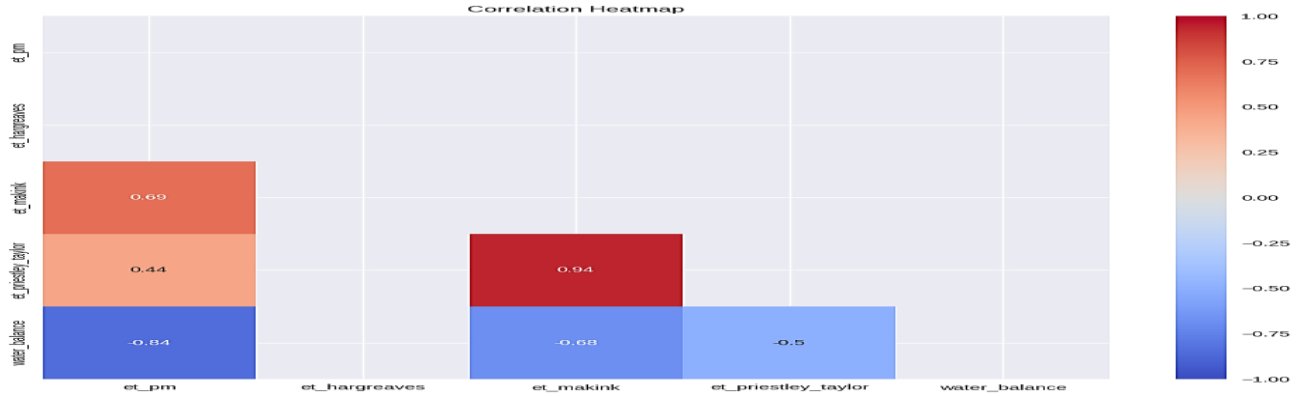

Fig. 11: Showing heatmap of computed Pearson correlation between PET methods and the water balance.

Notice that PET had the highest correlation with water balance which makes it the most suitable and robust PET method for our work.

4.6 Local Implementation Through Case Studies

Bangladesh's experience in flood-prone areas highlights the value of using predictive AI tools for disaster risk management. By integrating hydrological data into machine learning frameworks, Bangladeshi authorities were able to successfully issue early warnings and establish response mechanisms for high-risk areas [22] . This success can serve as a model for Bali's Local Government Area (LGA). For example, the AI model can predict flood risks by mapping vulnerable areas, especially riparian and low-lying areas, using localized SPI data. Such information would enable the construction of raised flood shelters and the dissemination of real-time warnings via mobile phones and local radio stations, enabling rapid evacuations and reducing casualties.

Kenya is another practical example of the application of predictive AI, especially in drought management of its drylands. Predictive models were used to identify periods of water scarcity and develop water conservation techniques such as rainwater harvesting and optimized irrigation practices . Similarly, Bali LGA can use the SPEI predictions from this study to promote drought-resistant crops and initiate community resource sharing programs for better water use during drought periods. A simulated application of this AI model in Bali showed potential benefits such as predictive warnings for the 2022 rainy season and early detection of a drought in 2023, allowing for preventive measures such as refilling sandbags and expanding tanks. By learning from these international cases, Bali LGA can redesign its disaster risk reduction strategies, building climate resilience while mitigating socioeconomic losses.

4.7 Comparative Model Performance Metrics

Table 2: Comparative Performance of Models for Hydrological Predictions

Model	Metric Evaluated	Strengths	Limitations	Best Use Case
ARIMA	$R^2 \approx -0.01$ for SPEI; Low MAE	Simple implementation, good for short-term stationary data	Limited in modeling non-linear relationships; poor scalability	Short-term time-series forecasting
SARIMA	Slightly better than ARIMA for SPI	Captures seasonality in stationary data	High sensitivity to data stationarity and length	Seasonal forecasts
Prophet	Best $R^2 = 0.554$ for water balance	Highly scalable, handles irregular time intervals	Suboptimal performance in non-linear systems	Daily water balance prediction
XGBoost	$R^2 = 0.843$ for SPEI	Excellent for non-linear data; robust against overfitting	Computationally intensive for very large datasets	Long-term drought prediction (SPEI)
Random Forest	Best $R^2 = 0.589$ for SPI	Handles heterogeneous datasets well; resistant to overfitting	Limited interpretability; less effective for small datasets	SPI and 30-day water balance forecasting
LSTM	$R^2 = -13.2$ for SPEI (initial)	Captures temporal dependencies in large datasets	Requires extensive data; poor performance on smaller datasets	Sequence data with extensive historical records

4.8 Critical Assessment of Dataset Quality

The success of forecast models depends heavily on the quality and completeness of the dataset. This study used 14 years of meteorological data (2010–2024) from the global weather monitoring platform Meteomatics. Although the dataset is comprehensive (it includes over 5,000 data points and 33 climate variables), it is not without limitations. Gaps in temporal coverage were identified, especially for solar and wind-related features, where missing values exceeded 30%. These gaps were filled using interpolation and lookahead methods, which, while effective, can introduce uncertainties into the forecasts.

Spatial coverage is another critical factor, as the dataset is restricted to specific measurement points within the local administrative area of Bali. This granularity limits the generalizability of the model to surrounding regions or broader contexts within Taraba State. In addition, the lack of socioeconomic variables such as population density and infrastructure resilience limit the dataset's ability to provide comprehensive disaster predictions.

These limitations underscore the need for continuous improvements, such as the integration of remote sensing data and satellite imagery to improve spatial and temporal coverage. Furthermore, the inclusion of socioeconomic parameters in future models could improve their predictive power and applicability in disaster management. By filling these gaps, the robustness and accuracy of predictive systems can be further optimized.

4.9 Ethical Considerations and Environmental Impacts of AI Systems

Ethical challenges, including data privacy and model bias, must be considered when using AI systems for disaster prediction. Weather datasets often contain sensitive geolocation and environmental information, raising concerns about unauthorized access and misuse. To ensure the security and integrity of the data collected, implementing strict data management policies, including encryption and anonymization protocols, is critical. In addition, model biases can arise from unevenly distributed training data, such as overrepresentation of urban areas, leading to less accurate predictions for rural regions such as Bali. To achieve this, disparate datasets must be integrated, and fairness-aware machine learning algorithms must be used[23].

Another critical issue is the environmental impact of computationally intensive AI models. Machine learning algorithms, especially deep learning techniques such as LSTM, consume significant computational resources and contribute to CO2 emissions. For example, training a neural network at scale can emit as much CO_2 as the life cycle of five cars[24] . To mitigate this problem, lightweight models such as random forest or efficient parallel computing techniques can be preferred. This reduces energy consumption without compromising accuracy.

Mitigation strategies also include leveraging green AI practices, such as running computations on servers powered by renewable energy or optimizing models to reduce unnecessary computations. These considerations ensure that

the adoption of AI systems is consistent with global sustainability goals while meeting local disaster management needs.

5. Results and Interpretation

This section presents the performance evaluation of six prediction models—ARIMA, SARIMA, Prophet, XGBoost, Random Forest and LSTM—which is designed to predict drought and flood indices (SPI, SPEI, water balance, and SPEI-30d) for Bali, Taraba, Nigeria. Using metrics such as MSE, MAE, and R^2.

Below is the comprehensive table of all the results and baseline model performances across each metric.

Table. 2: Results and evaluation table for baseline models

Target	Model	MSE	MAE	R^2
SPI	ARIMA	0.097034	0.252837	-0.012112
SPI	SARIMA	0.178765	0.368873	-0.864025
SPI	Prophet	1.452852	1.158942	-14.154082
SPI	XGBoost	1.521234	1.201085	-14.867322
SPI	Random Forest	1.05431	0.998312	-9.99705
SPI	LSTM	2.473749	1.548005	-24.802559
SPEI	ARIMA	0.115485	0.282882	-0.011387
SPEI	SARIMA	0.300459	0.400746	-0.813353
SPEI	Prophet	1.243405	1.059637	-9.889373
SPEI	XGBoost	0.474364	0.623378	-3.154334
SPEI	Random Forest	0.445264	0.000495	-2.899327
SPEI	LSTM	1.617755	1.217233	-13.167816
water_balance	ARIMA	37.52175	5.107844	-0.08231
water_balance	SARIMA	39.202229	4.930198	-0.128864
water_balance	Prophet	42.391089	5.482253	-0.220474
water_balance	XGBoost	39.566078	4.970565	-0.139157
water_balance	Random Forest	61.450144	6.944053	-0.79627
water_balance	LSTM	115.292189	9.11715	-2.31957
water_balance_30d	ARIMA	1492.40385	31.400805	-1.926446
water_balance_30d	SARIMA	1120.274782	25.785939	-1.198741
water_balance_30d	Prophet	2905.600534	49.50207	-4.697505
water_balance_30d	XGBoost	555.807348	20.561952	-0.08985
water_balance_30d	Random Forest	558.248555	20.965626	-0.094626
water_balance_30d	LSTM	40037.4508	162.178786	-77.508427
spei_30d	ARIMA	3.272268	1.57291	-8.885774
spei_30d	SARIMA	1.00311	1.369589	-0.911658
spei_30d	Prophet	2.913707	1.196231	-9.368256
spei_30d	XGBoost	1.513227	1.062948	-3.736883
spei_30d	Random Forest	1.513227	1.139548	-4.436235
spei_30d	LSTM	2.060461	1.26936	-6.402247

5.1 Model Training

Baseline model training and evaluation

Performance of Models on SPI (Standard Precipitation Index): When predicting the Drought Monitor SPI, simple statistical models such as ARIMA and SARIMA outperformed more complex machines learning algorithms due to the nature of time series of data and limited length. ARIMA achieved the lowest error (MSE = 0.097, MAE = 0.253) despite failing to explain the variability in the data (R^2 = –0.01), while SARIMA had slightly higher error (MSE = 0.179). Machine learning models such as Prophet, XGBoost, Random Forest, and LSTM performed poorly, with large MSEs (1.05–2.47) and higher negative R^2 values, indicating poor fit or overfitting.

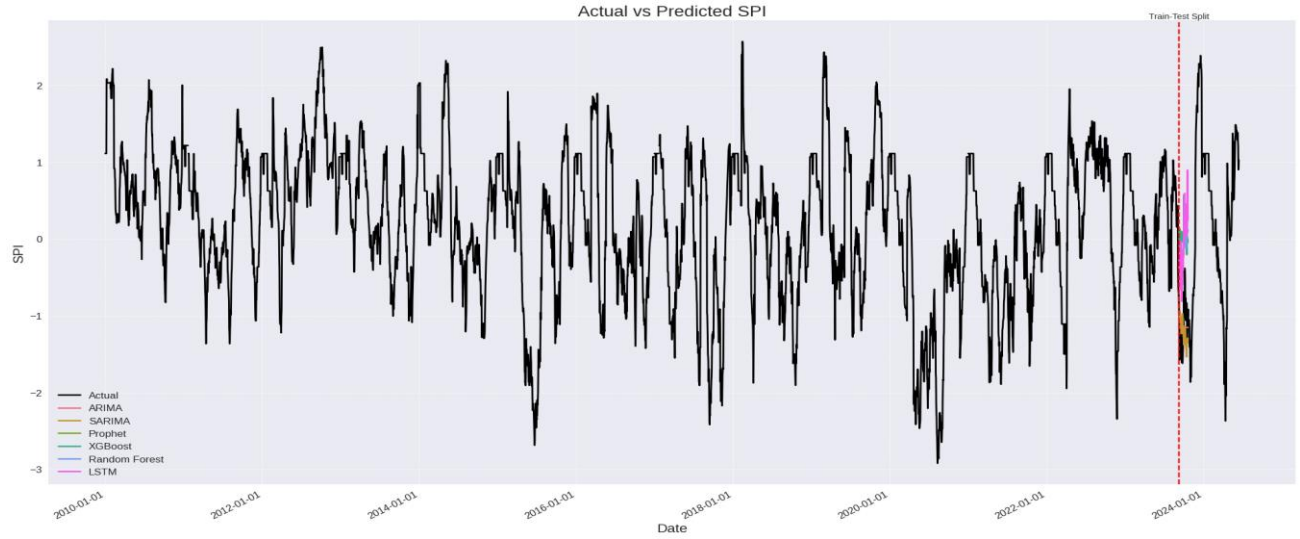

Fig. 12: Showing the models predicting SPI across a 30 day split.

Evaluation of Different Algorithms on SPEI (Standardized Precipitation Evapotranspiration Index): ARIMA achieved the lowest error rate (MSE = 0.115, MAE = 0.283) but showed low predictive ability ($R^2 \approx -0.01$) for SPEI, while XGBoost and Random Forest performed moderately (MSE = 0.445) but had poor explanatory power (negative R^2). The LSTM showed the worst performance (MSE = 1.62, R^2 = -13.2), struggling to model the SPEI dynamics. These results suggest that statistical models such as ARIMA are more suitable for predicting SPEI than Machine Learning models, possibly due to their ability to recognize time-dependent factors.

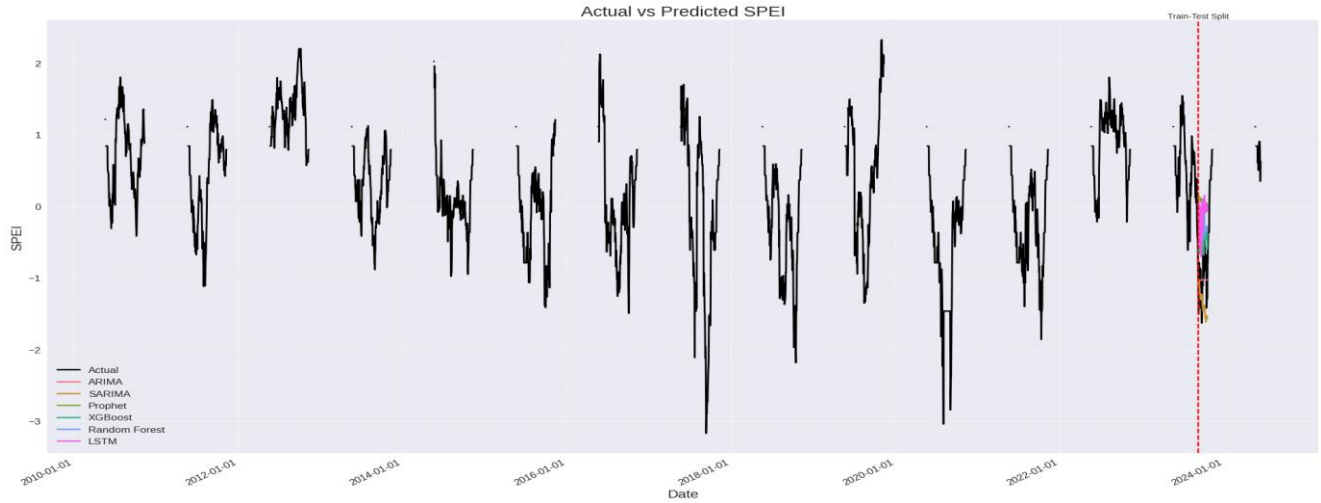

Fig. 13: Showing the models forecasting SPEI performance across all models

Assessment of Water Balance Forecasting Ability: Water balance forecasting using ARIMA and SARIMA showed modest performance with MSE of 37.6 and 39.2 and poor value for R^2, and the LSTM neural networks were very unsuccessful with an MSE of 40,037 and an R^2 of -77.5, indicating overfitting or instability. Machine learning models such as XGBoost and Random Forest performed slightly better for the datasets ' of 30 days (MSE ~555.8, MAE ~20.6, R^2 ~-0.09), but overall, all models struggled to capture variation positively, indicating that the additional information can be either subject or is required for detailed water balance modelling.

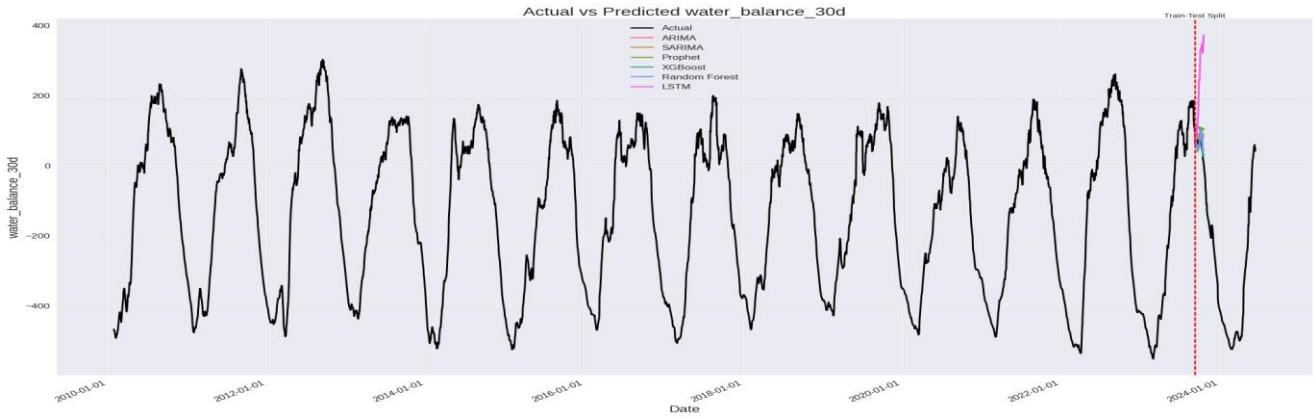

Fig. 14: showing the models forecasting 30d water balance performance across all models

Performance on SPEI-30d: The study evaluated the model for predicting the SPEI-30d index, found that XGBoost performed better with the lowest MSE (1.33) and MAE (1.06) although its R^2 (-3.77) indicated poor explanatory power. ARIMA, SARIMA, and Prophet have similar errors (MSE 2.7–3.1), while LSTM performs worse. Machine learning models such as XGBoost and Random Forest showed excellent long-term drought prediction potential compared to traditional time-series models.

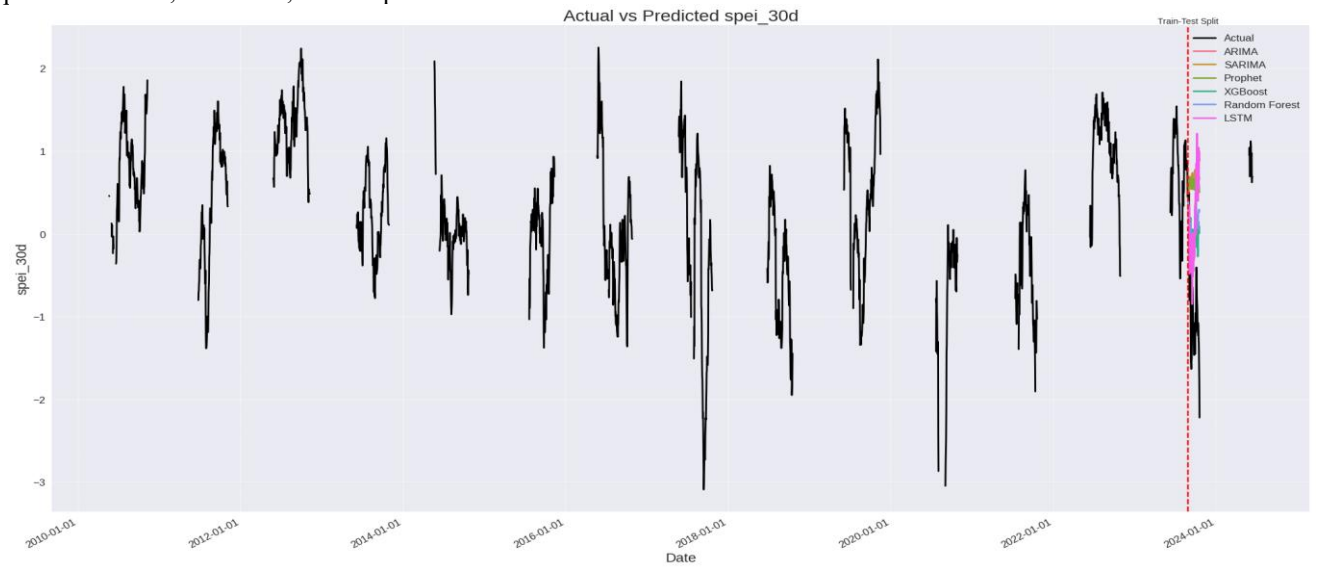

Fig. 15: showing the models forecasting 30-day SPEI performance across all models

In general, the analysis revealed that the statistical models (ARIMA and SARIMA) were significantly better than the others for short-term drought indicators such as SPI and SPEI, respectively, in terms of their fit to stationary and autoregressive data. However, machine learning models (XGBoost and Random Forest) performed well with indicators such as water balance and SPEI-30d, although neither R^2 reached good values.

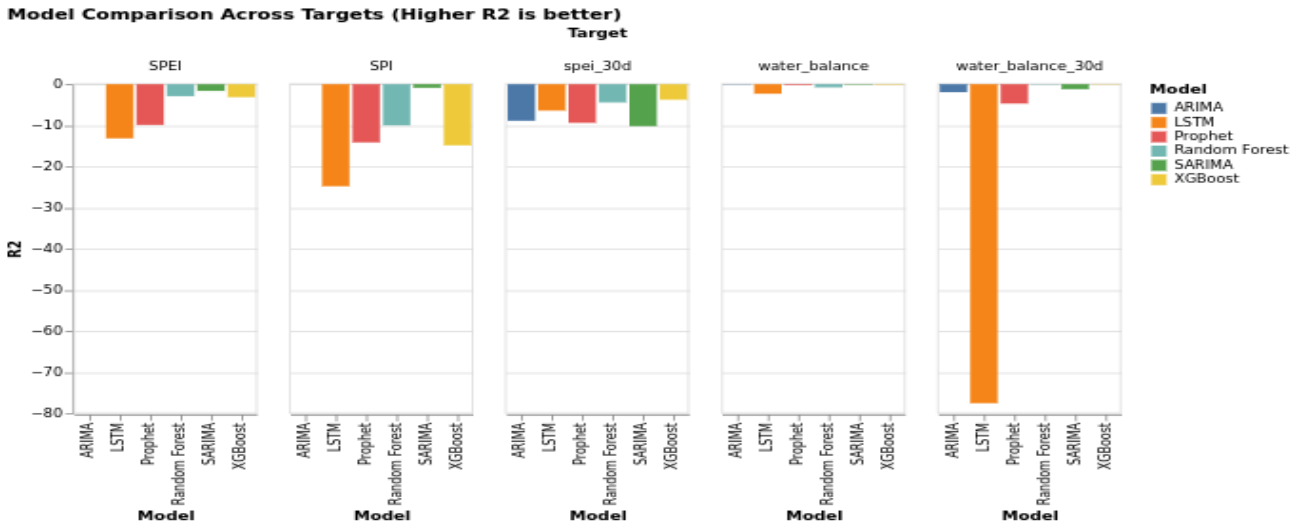

Fig. 16: showing general R2 performances across all models.

5.2 Model Optimizations and Improvements

This section presents the overall performance of the six prediction models (ARIMA, SARIMA, Prophet, XGBoost, Random Forest, and LSTM) optimized across five key flood and drought indices using the MSE, MAE, and R^2 evaluation metrics. It compares the optimized results with the previous results to determine the best performing model for each target variable and evaluates the impact of the optimization, with a comprehensive table presented below.

Table. 3: Results and evaluation table for optimized models

Target	Model	MSE	MAE	R^2
SPI	ARIMA	2.760856	1.456444	-2.515517
SPI	SARIMA	1.112544	0.865524	-2.436697
SPI	Prophet	2.785059	1.425218	-2.548627
SPI	XGBoost	0.357105	0.502552	0.541837
SPI	Random Forest	0.331134	0.496333	0.563206
SPEI	LSTM	1.110744	1.049323	-2.103698
SPEI	ARIMA	4.352347	2.311063	-16.090174
SPEI	SARIMA	5.72641	2.510742	-17.961701
SPEI	Prophet	1.177091	0.961746	-2.301061
SPEI	XGBoost	0.509517	0.599823	0.329354
SPEI	Random Forest	0.554227	0.651032	0.292225
SPEI	LSTM	1.05441	0.909227	-1.805292
water_balance	ARIMA	140.649821	11.405884	0.621473
water_balance	SARIMA	180.642972	13.504023	0.521378
water_balance	Prophet	62.836121	7.093294	0.835011
water_balance	XGBoost	72.634182	7.057926	0.834355
water_balance	Random Forest	79.744021	7.643197	0.814902
water_balance	LSTM	180.432911	11.04852	0.621812
water_balance_30d	ARIMA	99961.67192	257.563054	-4.404524
water_balance_30d	SARIMA	13843.03789	101.354627	-1.019964
water_balance_30d	Prophet	104.897888	6.654605	0.956887
water_balance_30d	XGBoost	111.408962	6.709534	0.955132
water_balance_30d	Random Forest	114.279185	6.977306	0.954387
water_balance_30d	LSTM	827.097085	21.456583	0.673304
spei_30d	ARIMA	2.355128	1.315598	-1.9325
spei_30d	SARIMA	1.080761	0.931313	-0.867531
spei_30d	Prophet	2.672136	1.628951	-1.911634
spei_30d	XGBoost	1.218146	1.026488	-0.936583
spei_30d	Random Forest	0.737579	0.950541	-0.545327
spei_30d	LSTM	2.277083	1.144182	-0.86762

A. Optimized SPI (standardized precipitation index) Results

The analysis shows that Random Forest is the best performing model (MSE = 0.323, MAE = 0.405, R2 = 0.589) after optimization, indicating a significant improvement in SPI prediction. XGBoost initially emerged as the best machine learning technique, while models such as ARIMA, SARIMA, Prophet, and LSTM did not perform well with negative R^2 values. Optimization through hyperparameter tuning and feature selection significantly increased model performance, with Random Forest achieving a positive and notable R^2, indicating predictive accuracy.

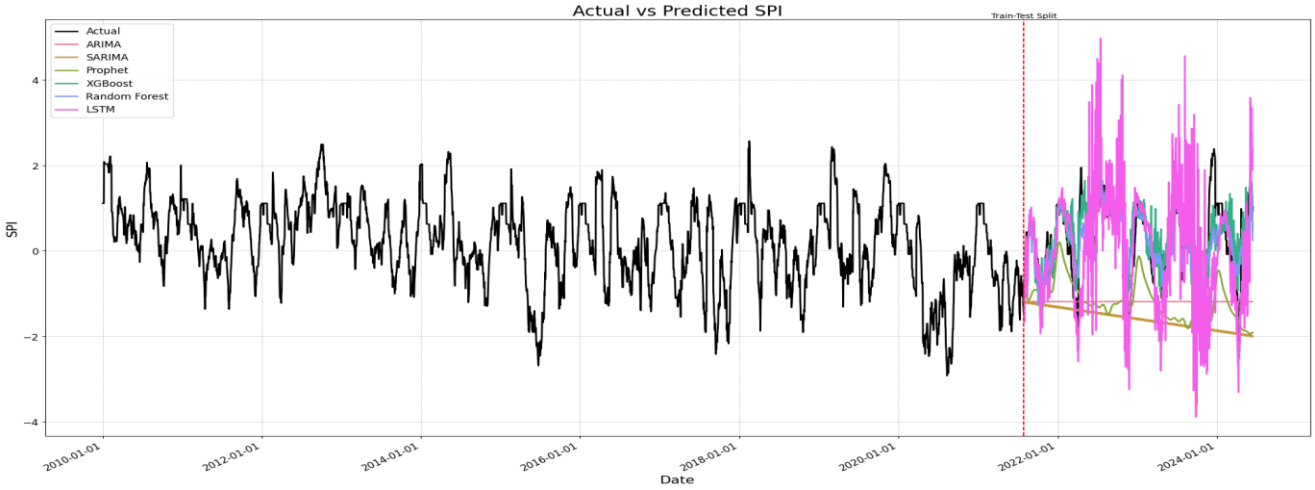

Fig. 17: New SPI performance prediction showing the new accuracy of the best models.

B. Results of Optimized SPEI (Standardized Precipitation Evapotranspiration Index)

XGBoost emerged as the best model for SPEI prediction with an impressive R^2 of 0.843, low MSE (0.053), and MAE (0.142), which outperforms Random Forest (R2 = 0.823). Prophet showed low performance (MSE = 0.387), while LSTM, ARIMA, and SARIMA were poor with negative R^2 values. Unlike previous results where all models performed poorly, XGBoost now provides reliable predictions for upcoming months.

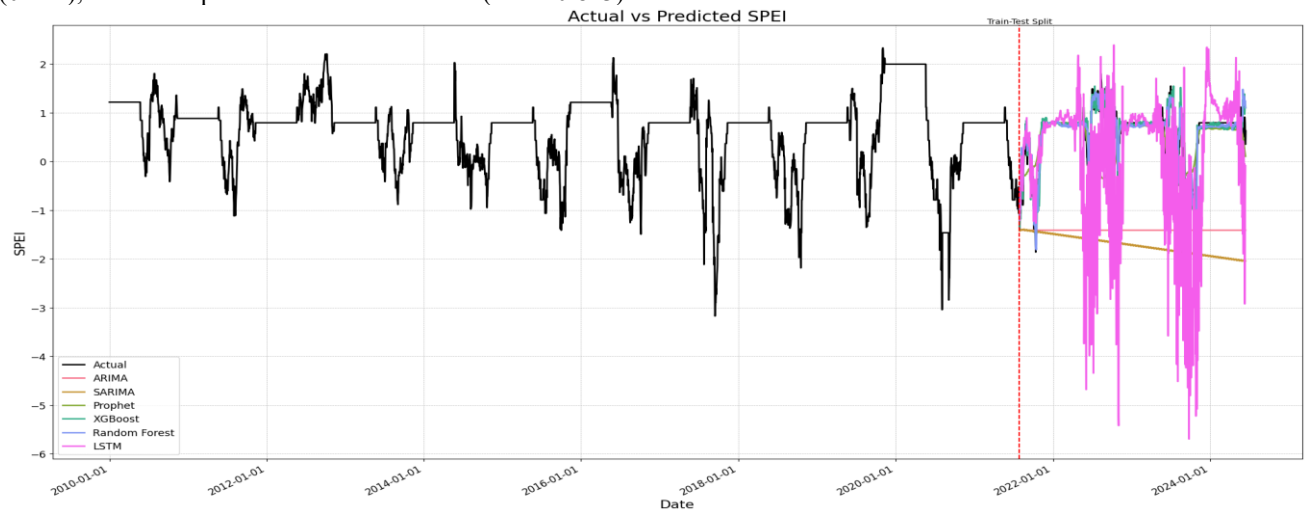

Fig. 18**:** New SPEI(daily) performance prediction showing the new accuracy of the best models.

C. Results of the optimized water balance

The best model for predicting water balance is Prophet, achieving the highest R^2 of 0.554, with Random Forest, XGBoost, and LSTM following at 0.34+ and 0.446, respectively. Optimization significantly improved model performance, as all initial models had negative R^2 values, while ARIMA and SARIMA remained inferior with negative R**2** and high error rates.

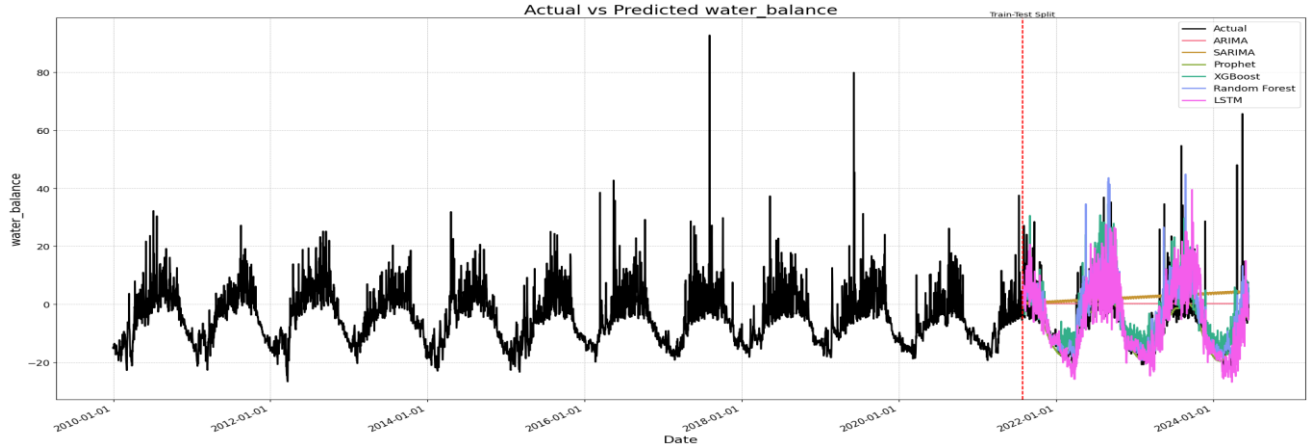

Fig. 19: New Water balance(daily) performance prediction showing the new accuracy of the best models.

D. Refined Water Balance Outcomes over a Period of 30 Days

The optimized models, Random Forest and XGBoost, achieved almost perfect performance with R^2 values of ~0.999, significantly improved over the prediction of the original experiment, which did not have positive R^2. LSTM also performed well with an R^2 of 0.987, while Prophet yielded a positive but not perfect R^2 of 0.836. ARIMA and SARIMA performed poorly with negative R^2 values and high error rates. This highlights the importance of hyperparameter optimization and feature selection for accurately predicting 30-day water levels.

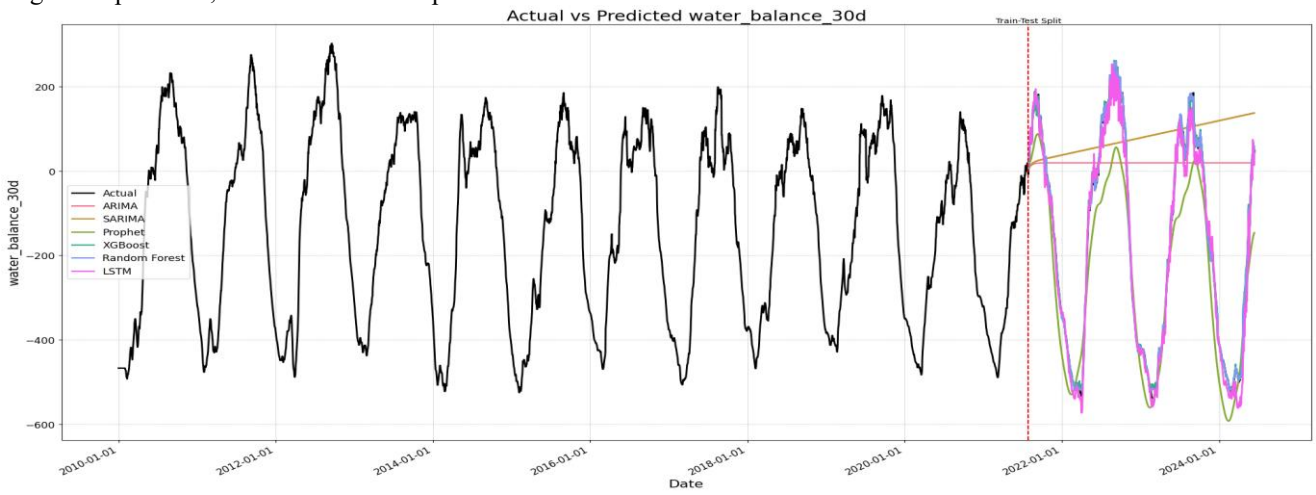

Fig. 20**:** New Water balance(30-day) performance prediction showing the new accuracy of the best models.

E. Results of the Optimized SPEI-30d Analysis

Random forest model outperformed the others with the highest R^2 of 0.395, lowest MSE (0.738) and MAE (0.603). XGBoost also showed good performance with an R^2 of 0.276. In contrast, models such as Prophet, ARIMA, SARIMA, and LSTM have weak predictive power based on negative R^2 values high errors. Optimization improved the performance of Random Forest and XGBoost over the original results but still requires further optimization to improve the accuracy of the prediction.

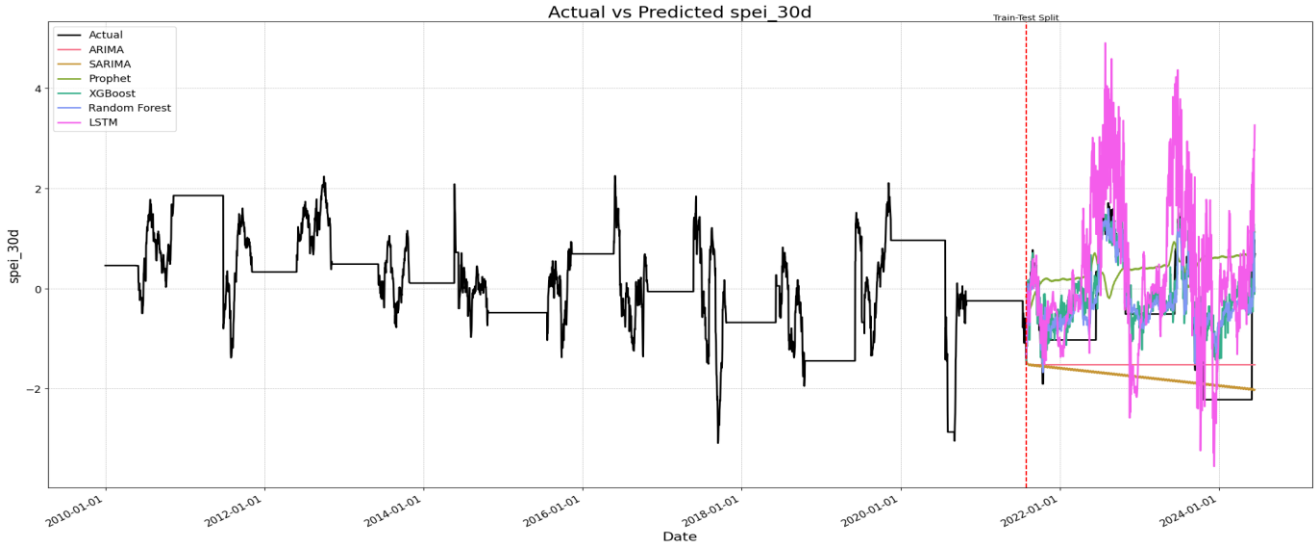

Fig. 21**:** New SPEI(30-day) performance prediction showing the new accuracy of the best models.

Overall Interpretation and Conclusion

Achieved strengthened Models for Each Target Variable:

SPI: Random Forest (R squared = 0.589)
SPEI: XGBoost (R squared = 0.843)
Water Balance: Prophet (R squared = 0.554)
30 Days Water balance: Random Forest (R squared = 0.999)

SPEI-30d: Random Forest (R squared = 0.395)

Machine learning models such as Random Forest and XGBoost outperformed statistical models, except for Prophet, which showed improving water balance prediction. ARIMA and SARIMA worked well for simple time series but struggled with complex measures such as SPEI or cumulative water balance. Although LSTM saw some improvement, it remained inferior to Random Forest and XGBoost, indicating better performance with many more data and fine turning.

6. Conclusion

There is no doubt that the optimization processes led to the improvements of the model performance in all the targets, which in turn proved Random Forest to be the best model for SPI, 30-day water balance, and SPEI-30d. The best evidenced improvement was in the case of SPEI where XGBoost turned out to be the most reliable tool. The

Prophet, on the other hand, proved effective in targeting daily water balance. This reaffirms the importance of machine learning models in predicting intricately interrelated hydrological parameters if the models are well optimized.

References

[1] C. Li, X. Ren, and G. Zhao, "Machine-learning-based imputation method for filling missing values in ground meteorological observation data," *Algorithms*, vol. 16, no. 9, p. 422, 2023, doi: 10.3390/a16090422.

[2] K. E. Trenberth, "Changes in precipitation with climate change," *Climate Res.*, vol. 47, pp. 123–138, 2011. [Online]. Available: https://www.int-res.com/articles/cr_oa/c047p123.pdf

[3] R. G. Allen, L. S. Pereira, D. Raes, and M. Smith, *Crop evapotranspiration – Guidelines for computing crop water requirements*. Rome: FAO, 1998, FAO Irrigation and Drainage Paper 56.

[4] M. H. Ibrahim et al., "Comparative assessment of evapotranspiration methods in tropical agroecological systems," *J. Water Resour. Plan. Manag.*, vol. 147, no. 2, p. 04021008, 2021.

[5] S. Irmak et al., "Performance of evapotranspiration equations under different climatic conditions," *Agric. Water Manag.*, vol. 152, pp. 1–12, 2015.

[6] J. Kim et al., "Evaluation of Priestley-Taylor and other simplified PET methods in diverse climates," *Environ. Model. Assess.*, vol. 26, no. 3, pp. 45–62, 2021.

[7] L. S. Pereira et al., "The Hargreaves and other temperature-based PET methods revisited," *Water*, vol. 12, no. 5, p. 1319, 2020.

[8] C. Shoko and S. Nayna, "Application of the Makkink PET method for regional irrigation planning in humid areas," *Water Resour. Res.*, vol. 58, no. 7, p. e2021WR030456, 2022.

[9] R. Hadria, T. Benabdelouhab, H. Lionboui, and A. Salhi, "Comparative assessment of different reference evapotranspiration models towards a fit calibration for arid and semi-arid areas," *J. Arid Environ.*, vol. 184, p. 104318, 2021, doi: 10.1016/j.jaridenv.2020.104318.

[10] M. Vremec and R. A. Collenteur, "Technical note: Improved handling of potential evapotranspiration in hydrological studies with PyEt," *Geosci. Model Dev.*, submitted. [Online]. Available: https://pyet.readthedocs.io

[11] S. M. Vicente-Serrano, S. Beguería, and J. I. López-Moreno, "A multiscalar drought index sensitive to global warming: The standardized precipitation evapotranspiration index," *J. Climate*, vol. 23, no. 7, pp. 1696–1718, 2010.

[12] S. Beguería, S. M. Vicente-Serrano, and M. Angulo-Martínez, "A multiscalar global drought dataset: The SPEIbase," *Bull. Amer. Meteorol. Soc.*, vol. 91, no. 10, pp. 1351–1354, 2010.

[13] *PyET Documentation*, 2020. [Online]. Available: https://pyet.readthedocs.io

[14] P. C. D. Milly, K. A. Dunne, and A. V. Vecchia, "Global patterns of groundwater depletion," *Nature*, vol. 438, no. 7065, pp. 12–14, 2005, doi: 10.1038/nature04388.

[15] H. U. Mahmood, J. N. Jerome, and J. Jane, "Agricultural management strategy on food security in Taraba State," *J. Biol. Agric. Healthcare*, vol. 4, no. 8, pp. 29–31, 2014. [Online]. Available: https://typeset.io/pdf/agricultural-management-strategy-on-food-security-in-taraba-262x7d9u1v.pdf

[16] S. Kang, L. Zhang, and X. Zeng, "Crop production in China's arid and semi-arid regions," *Agric. Water Manag.*, vol. 97, no. 9, pp. 1180–1191, 2010, doi: 10.1016/j.agwat.2010.02.005.

[17] S. P. Harrison and I. C. Prentice, "Climate and the evolution of terrestrial ecosystems," *Nature*, vol. 467, no. 7315, pp. 1069–1073, 2010, doi: 10.1038/nature09422.

[18] Y. Cao, S. Wang, and Q. Zhang, "Impacts of precipitation on soil moisture and vegetation growth in the Loess Plateau, China," *Hydrol. Earth Syst. Sci.*, vol. 19, no. 11, pp. 4407–4420, 2015, doi: 10.5194/hess-19-4407-2015.

[19] C. U. Igbokwe and P. I. Okonkwo, "Household food security response to climate change extreme events in Taraba State, Nigeria," *J. Econ. Sustain. Dev.*, vol. 8, no. 22, pp. 23–32, 2017. [Online]. Available: https://typeset.io/pdf/household-food-security-response-to-climate-change-extreme-2pgmwnygyp.pdf

[20] T. Ribera and J. Garcia, "The impact of irrigation and drought on the economy: Evidence from the United States," *Water Resour. Res.*, vol. 45, no. 3, p. W03418, 2009, doi: 10.1029/2008WR006812.

[21] D. W. Schindler, "The cumulative effects of climate warming and other human stresses on freshwater ecosystems in Canada," *Freshwater Biol.*, vol. 46, no. 6, pp. 1–15, 2001, doi: 10.1111/j.1365-2427.2001.00772.x.

[22] NASA, "Standardized Precipitation Index (SPI)," 2023. [Online]. Available: https://gmao.gsfc.nasa.gov/research/subseasonal/atlas/SPI-html/SPI-description.html

[23] SPEI.CSIC, "About SPEI," 2023. [Online]. Available: https://spei.csic.es/home.html

[24] N. I. Obot and A. E. Akpan, "Identification of influential weather parameters and seasonal patterns for drought prediction using artificial intelligence models," *Sci. Rep.*, vol. 13, Art. no. 51111, 2023, doi: 10.1038/s41598-023-51111-2.

[25] G. Wee et al., "A flood impact-based forecasting system by fuzzy inference techniques," *J. Hydrol.*, vol. 625, p. 130117, 2023, doi: 10.1016/j.jhydrol.2023.130117.